Cite as: R. V. Jagadeesh *et al.*, *Science* 10.1126/science.aan6245 (2017).

# MOF-derived cobalt nanoparticles catalyze a general synthesis of amines

**Rajenahally V. Jagadeesh,[1]* Kathiravan Murugesan,[1]* Ahmad S. Alshammari,[2] Helfried Neumann,[1] Marga-Martina Pohl,[1] Jörg Radnik,[1] Matthias Beller[1]†**

[1]Leibniz-Institut für Katalyse e.V. an der Universität Rostock, Albert-Einstein Strasse 29a, Rostock, D-18059, Germany. [2]King Abdulaziz City for Science and Technology, Post Office Box 6086, Riyadh 11442, Saudi Arabia.

*These authors contributed equally to this work.

†Corresponding author. Email: matthias.beller@catalysis.de

**The development of base metal catalysts for the synthesis of pharmaceutically relevant compounds remains an important goal of chemical research. Here, we report that cobalt nanoparticles encapsulated by a graphitic shell are broadly effective reductive amination catalysts. Their convenient and practical preparation entailed template assembly of cobalt-diamine-dicarboxylic acid metal organic frameworks on carbon and subsequent pyrolysis under inert atmosphere. The resulting stable and reusable catalysts were active for synthesis of primary, secondary, tertiary and *N*-methylamines (>140 examples). The reaction couples easily accessible carbonyl compounds (aldehydes, ketones) with ammonia, amines or nitro compounds and molecular hydrogen under industrially viable and scalable conditions, offering cost-effective access to numerous amines, amino acid derivatives, and more complex drug targets.**

The development of nanostructured catalysts for innovative organic synthesis is crucial for the advancement of sustainable processes in the chemical, pharmaceutical and agrochemical industries (*1–8*). However, most of the nanocatalysts known to date were developed for the activation of structurally simple molecules (*3–8*) and are scarcely applied for more challenging synthetic reactions or refinement of structurally complex compounds. Among the different classes of nanomaterials, supported metal particles are particularly valued for their low energy consumption and high activities and selectivities (*1–14*), which can be tuned by controlling the nature, size, distribution and stability of the nanoparticles as well as surface composition of the support (*9–14*). In general, simple supported metal nanoparticles are prepared by thermal (via pyrolysis or calcination) or chemical reduction of the respective metal salts on heterogeneous supports (*1–10*). To improve the activity of these simple materials, well-defined organometallic complexes have also recently been explored as precursors for pyrolytic activation (*13*, *14*). Although the resulting materials found application in catalytic hydrogenations and oxidations (*13*, *14*), they largely exhibit poor reactivity and selectivity for other challenging synthetic organic reactions. One key to more rational preparation of active nanoparticulate catalysts might be the use of structure-controlling templates, which should strongly bind to the respective metal ions. In this respect, metal organic frameworks (MOFs) represent a stable class of porous compounds, which can be assembled in a highly modular manner from metal ions and organic linkers (*15–17*). Recently, they have been used as self-sacrificing compounds for producing bulk materials by their direct pyrolysis without the use of external heterogeneous supports (*18–23*). Here, we describe the use of MOFs as specific precursors for producing highly active and stable cobalt nanoparticles supported on commercial carbon. In contrast to previous works (*18–23*), the pre-formed material (cobalt-diamine-dicarboxylic acid MOF) acted as a structure directing template for pyrolysis on carbon. Compared to more conventional routes to heterogeneous materials prepared by impregnation or immobilization, in our procedure the pyrolysis precursor is better defined. We applied the resulting nanoparticles to reductive amination of carbonyl compounds for the general synthesis of amines.

Amines represent a privileged class of compounds used extensively in fine and bulk chemicals, pharmaceuticals and materials (*24–29*). In fact, 170 of the top 200 drugs of 2015 contained nitrogen and/or amino groups (*26*). Catalytic reductive amination of carbonyl compounds with molecular hydrogen is widely performed in research laboratories and industrial facilities (*30–48*). However, the preparation of primary amines using ammonia relies on either precious metal-based catalysts (*30*, *31*, *33–39*) or Raney nickel (*30*, *31*, *40*), which often remains non-selective or otherwise problematic (*30*, *31*, *34–40*). Hence, the development of more selective and earth-abundant metal-based catalysts continues to attract scientific interest.

Downloaded from http://science.sciencemag.org/ on September 21, 2017

### Preparation of MOF-derived cobalt nanoparticle-based catalysts

We initially explored MOFs assembled in dimethylformamide (DMF) at 150°C from iron, manganese, cobalt, nickel or copper nitrates and organic linkers 1,4-diazabicyclo[2.2.2]octane (DABCO) and terephthalic acid (TPA). Next, these in situ generated MOFs were immobilized on commercial Vulcan XC 72R carbon powder. Upon slow evaporation of the solvent followed by drying of the resulting MOFs, the template on carbon was formed (Fig. 1). Subsequent pyrolysis at 800°C for 2h under argon atmosphere produced the final nanoparticles. In addition, the Co-DABCO-TPA MOF was separately prepared and isolated prior to pyrolysis on carbon (see supplementary material S2.2 for detailed preparation). Hereafter, all these materials are labeled as M-L1-L2@C-x, where M = Fe, Mn, Co, Ni, Cu; L1 = DABCO; and L2 = TPA and x denotes the pyrolysis temperature, respectively.

All of these materials were tested in the benchmark reductive amination of 3,4-dimethoxybenzaldehyde using ammonia and hydrogen to give veratrylamine (3,4-dimethoxybenzylamine), which is present as a structural motif in several bioactive molecules. As shown in fig. S1, materials resulting from pyrolysis of Fe-, Mn-, Cu- and Ni-DABCO-TPA@C at 800°C showed no or only little catalytic activity. Gratifyingly, the corresponding cobalt catalyst (Co-DABCO-TPA@C-800) from Co-MOFs gave a very good yield (88%) of the desired amine. The pyrolyzed materials prepared from the in situ generated and the isolated Co-MOFs exhibited similar activity. Pyrolysis of cobalt nitrate with either DABCO (Co-DABCO@C-800) or TPA (Co-TPA@C-800) linkers alone led to less active catalysts (15-20% yields). Apart from the metal and the linkers, the pyrolysis temperature was important for activity. Specifically, pyrolysis at 400°C gave material with poor reactivity (16% yield), whereas pyrolysis at 600°C and 1000°C resulted in active catalysts (75% and 83% yields, respectively). As expected, the homogeneous catalyst and the pyrolyzed cobalt nitrate ($Co(NO_3)_2$@C-800) were not active. Similarly, the Co-MOFs with and without support showed no product formation (fig. S1).

### Characterization of cobalt nanoparticle-based catalysts

We undertook detailed structural characterization of these cobalt-based catalysts. Aberration-corrected scanning transmission electron microscopy (STEM) analysis of the most active material (Co-DABCO-TPA@C-800) revealed the formation of mainly metallic cobalt particles with diameter ranging from less than 5 nm to 30 nm (Fig. 2). The energy-dispersive X-ray spectroscopy map (EDXS) (Fig. 2A left) shows mainly the presence of metallic Co particles within the carbon matrix. Most of these are surrounded by a combination of some graphitic layers and short-range ordered graphitic shells (Fig. 2A, middle). In addition, a smaller quantity of core-shell particles with cobalt oxide shells at metallic Co is also present (fig. S2A). In regions of short-range ordered carbon, we detected single Co atoms as bright dots in high angle annular dark field (HAADF) images (Fig. 2A, right). To get information on the cobalt/carbon/nitrogen relation the parallel mapping of EDXS for all elements and electron energy loss spectroscopy (EELS) (Fig. 2B) optimized for carbon, nitrogen and oxygen was performed. Because the nitrogen signal is superimposed on the carbon signal in EDXS, these maps were only used for the Co distribution. Figure 2B shows the maps of C, N and Co (left image) in the neighborhood of a metallic particle wrapped by graphitic carbon. The C/N overlay in the HAADF image (middle image) gives evidence that nitrogen is not only located in the graphitic shell on the Co particle but surprisingly in short range ordered carbon which is not part of the graphitic shell and corresponds to features with single atoms shown in Fig. 2A. Co traces are detectable everywhere in the nitrogen containing carbon at low concentration. In contrast, the less active material Co-DABCO@C-800 contained mainly hollow cobalt oxide ($Co_3O_4$) particles (fig.S2B). In addition to $Co_3O_4$, some Co-$Co_3O_4$ core-shell particles were also present. Although sub-nm Co structures are found in this material, no single Co atoms were detected. Similarly, Co-TPA@C-800 (fig. S2C) also contained mainly cobalt oxide ($Co_3O_4$) particles encapsulated within graphitic shells along with a small quantity of metallic cobalt in Co-$Co_3O_4$ core-shell structures. No single Co atoms or sub nm Co structures were detected in this material. Cobalt nitrate@C-800, which was completely inactive, contained hollow $Co_3O_4$ with short-range ordered carbon from the support in the vicinity (fig. S2D).

In order to understand the formation mechanism of the active catalyst, materials pyrolyzed at lower temperatures were also characterized (fig. S3). In Co-DABCO-TPA@C-400, a minor amount of metallic cobalt was present in the core of cobalt/cobalt oxide core-shell structures, and no formation of graphitic shells was observed. Co-DABCO-TPA@C-600 contained more metallic cobalt, and incipient formation of graphitic shells enveloping the metallic Co was evident. Apparently, this structural process is crucial for high activity and stability. For the most active Co-DABCO-TPA@C-800, single Co atoms within some of the graphitic structures were detected. In the case of Co-DABCO-TPA@C-1000, most of the Co was present in metallic crystallite morphology completely covered by graphitic structures. In all of the active catalysts, cloudy regions of cobalt species in the 1-2 nm range were detected. The different phases of cobalt in both active and less active catalysts have been also confirmed by x-ray powder diffraction data (figs. S7 and S8) that accorded with the TEM analysis.

Downloaded from http://science.sciencemag.org/ on September 21, 2017

The nature and quantity of nitrogen in these materials was further explored by x-ray photoelectron spectroscopy (XPS) (fig. S10 and S11). Surprisingly, the combination of the two linkers increased the quantity of nitrogen in the near-surface region significantly compared to either linker alone (fig. S12). The N content in Co-DABCO-TPA@C-800 was three times higher than in Co-DABCO@C-800, whereas in Co-TPA@C-800 only traces of N were observed. In both Co-DABCO-TPA@C-800 and Co-DABCO@C-800, two N-states could be detected (fig. S10): One correlating with imine-like N known from pyridine (ca. 398 eV) (*49*, *50*), the other manifesting a higher binding energy, corresponding to N bonded to the metal (*49*, *50*). For the former sample a clear separation of both peaks was observed due to the slightly higher binding energy. For Co-DABCO-TPA@C pyrolyzed at different temperatures, iminic N was observed and the binding energy of the Co-N bond increased as pyrolysis temperature ascended up to 800°C (fig. S11). In comparison to all other samples, the observation of the two N states was unique to these active systems (fig. S11) (*49*, *50*). It seems that for the optimal catalyst, the bonding between Co and N is most pronounced. In the material pyrolyzed at 1000°C the formation of nitrides could be observed, as well (fig. S11). In the un-pyrolyzed and 1000°C samples, the amount of Co in the near-surface region was too low for a reasonable peak fitting; for all other samples, the metal content was nearly the same.

**Synthesis of primary amines**

With an active material (Co-DABCO-TPA@C-800; hereafter represented as catalyst **I**) in hand, we investigated its substrate scope in the reductive amination. Initially, various primary amines, which are easily further functionalized and therefore represent central building blocks, were prepared starting from carbonyl compounds and simple ammonia (Figs. 3 and 4). A crucial problem for the synthesis of primary amines has been the subsequent formation of secondary and tertiary amines. The few catalysts known for the chemoselective reductive amination of aldehydes and ketones to give primary amines are based on precious metals (*30*, *31*, *34–39*) or Raney Ni (*30*, *31*, *40*). Although Raney nickel is available and comparably inexpensive, it is highly flammable, hazardous and less selective for functionalized and structurally complex molecules.

By applying our cobalt catalyst, we performed selective reductive amination of 38 aldehydes to produce benzylic, heterocyclic and aliphatic linear primary amines, in good to excellent yields (up to 92%) (Fig. 3). Sensitive functional groups including halides, esters as well as challenging carbon-carbon double and triple bonds were well tolerated. We also prepared amino-Salicin in 83% yield from the O-glucoside Helicin (Fig. 3; product 41) to showcase the selective amination of bio-active compounds. Compared to benzaldehydes, the reductive amination of aliphatic aldehydes is hampered by unproductive aldol condensation, which can easily occur under basic conditions. Nevertheless, several aliphatic and araliphatic substrates gave the corresponding primary amines in good yields (up to 92%) and high selectivity.

The hydrogenation of the in situ generated imine from aldehydes is faster than reduction of the corresponding ketone-derived imines. Thus, a more active catalyst or more drastic conditions tend to be required for efficient reductive amination of ketones. The generality of catalyst **I** was further demonstrated by the synthesis of branched primary amines starting from diverse ketones (Fig. 4). Gratifyingly, both industrially relevant and structurally challenging ketones underwent smooth amination and produced the corresponding primary amines in good to excellent yields (Fig. 4). Biologically active amphetamines (products **77-79**), which are potent central nervous system (CNS) stimulating drugs, were prepared in up to 91% yield. In general, amphetamines are synthesized by reductive amination of the corresponding phenyl-2-propanones using ammonium formate at higher temperature (Leuckart-Wallach reaction) (*51*). More sensitive products are prepared by reductive amination reactions using more expensive Pt- and Pd-based catalysts (*51*). We also explored amination of non-steroidal anti-inflammatory agents (**80-82**) and steroid derivatives (**83-87**). Introduction of amino groups into these bio-active molecules has been scarcely explored so far. Sulfur-containing compounds constitute a common poison for most heterogeneous catalysts, though they're found in more than 300 FDA-approved drugs (*52*). In this context, thioethers are the most common scaffolds. Gratifyingly, catalyst **I** tolerated several S-containing substrates including thiophene, thioether, and sulfone (Figs. 3 and 4; products **28, 29, 30, 43, 46, 50**).

**Synthesis of secondary and tertiary amines**

We next explored the synthesis of secondary and tertiary amines (Fig. 5), which are found in a large number of biologically active natural products (*26–29*). In contrast to the preparation of primary amines using ammonia (vide supra), a few non-noble-metal based catalysts have already been used for reductive aminations to prepare secondary and tertiary amines; however, in such cases functional group tolerance and broad substrate scope have been limited (*41–48*). Both nitroarenes and amines reacted with aldehydes to give the corresponding secondary amines selectively in up to 92% yields (Fig. 5A; products 88-103). Compared to the traditional reaction of anilines, the one-pot reductive amination of nitroarenes and carbonyl compounds is straightforward and ensures a better step economy. This direct process shows that the cobalt nanocatalyst can also be used for the selective hydrogenation of nitroarenes to anilines, which are of additional interest for dye formation and materials synthesis. The

Downloaded from http://science.sciencemag.org/ on September 21, 2017

reductive alkylation of *N*-containing heterocycles as well as primary and secondary amines gave the corresponding derivatives in 81-88% yields. To demonstrate the amination of ketones, phenyl-2-propanone was reacted with 4-aminocyclohexane or 4-aminocyclohexanol (aliphatic amines) and produced the corresponding secondary amines in 84% and 89%, respectively (Fig. 5A products 104 and 105). Further, we also tried the reductive amination of acetophenone using nitroarenes or aromatic amines, but did not observe any significant desired product formation in this case. Competition reactions of aniline with 4-bromobenzaldehyde and acetophenone were examined. Here, reductive amination of the aldehyde occurred with excellent conversion and high selectivity, while the ketone remained untouched. Similarly, the reaction of 4-bromobenzaldehyde with aniline proceeded selectively in the presence of phenyl-2-propanone. Thus, this catalyst allows for selective amination of aldehydes in the presence of ketones. In general, for the majority of reductive amination reactions high chemoselectivity is obtained. However, in a few cases we observed minor amounts of the corresponding alcohol (<5%), and/or secondary imine/amine (<10%). In the preparation of secondary amines, up to 10% of the imine was observed. In bromo-substituted substrates (products **6, 7, 89, 112, 117, 122, 125**), we also observed small amounts of de-halogenation. In general, we did not detect any over-alkylation products.

To demonstrate compatibility with pre-existing stereochemistry, we performed the reductive *N*-alkylation with chiral amines. A plethora of chiral amines is available from biological and industrial sources. As shown in Fig. 5B, the *N*-alkylations of (S)-(−)-1-methylbenzylamine and (R)-(+)-α-methylbenzylamine proceeded efficiently and offered the corresponding chiral amine derivatives with retention of the original stereochemistry (Fig. 5B; products 106-108), as assessed by chiral HPLC (see supplementary materials S6.4(a) for procedure and HPLC data). Further, the reductive alkylation of two amino acid esters (phenylalanine and tyrosine) was performed in 82-89% yields (Fig. 5C; products **109-114**). However, the chirality of these N-alkylated amino acid esters was not retained and we obtained the corresponding racemic mixtures.

### Synthesis of *N*-methylamines

Among the various alkylated amines, N-methylamines are of special interest, due to their role in regulating biological functions (*53*, *54*). In general, this class of amines is prepared either by Pd/C-catalyzed reductive amination with formaldehyde or by using active (toxic) methylation reagents. By applying our cobalt catalyst **I** we prepared selected *N*-methylamines starting from aldehydes and *N*,*N*-dimethylamine (DMA), which is also a readily available bulk chemical (Fig. 6A). In addition, the direct reductive methylation of nitroarenes or amines with aqueous formaldehyde produced selectively the corresponding *N*-methylamines (Fig. 6B). Compared to traditional alkylations using methyl-X compounds, advantageously the presented cobalt-catalyzed synthesis of *N*-methylamines is either more cost-effective or waste-free.

### Demonstrating catalyst recycling and gram scale reactions

Stability and recyclability are crucial features for any heterogeneous catalyst. In addition to the obvious cost advantages, the use of recyclable heterogeneous catalyst can considerably facilitate product purification. As shown in the reductive amination of phenylacetone our supported cobalt nanoparticles are highly stable and are conveniently recycled up to 6 times without any significant loss of catalytic activity (fig. S14). After that slight decrease of activity is observed.

Next, gram scale reactions were performed for several interesting substrates. Apart from amphetamine, related 4(-4-hydroxyphenyl)-2-amino-butane and 1, 1-diphenyl-2-aminopropane as well as 17-amino-estrone were synthesized in up to 50 g scale (Fig. 4). In all the cases similar yields to those of 50-100 mg scale reactions were obtained.

Finally, we undertook preparation of ten existing drug molecules (Fig. 5D). These syntheses showcase the applicability of the supported cobalt nanoparticles for selective preparation of amine-based drugs. Previously, these molecules were prepared by the reductive amination reactions using either precious metal-based catalysts or sodium borohydride (*55–59*). In addition, some have also been prepared by nucleophilic substitution reactions of corresponding amines with halogenated compounds (*55–60*). Here, the corresponding aromatic aldehydes were treated with piperazine and morpholine derivatives or primary amines to give the desired products in 82-92% yields according to our standard procedure, which further demonstrates the general utility of this single cobalt-based catalyst.

Downloaded from http://science.sciencemag.org/ on September 21, 2017

## REFERENCES AND NOTES


1. *Nanotechnologies: Principles, Applications, Implications and Hands-on Activities* (European Commission, European Union, 2012).
2. V. Polshettiwar, T. Asefa, *Nanocatalysis: Synthesis and Applications* (Wiely, 2013).
3. A. Corma, P. Serna, Chemoselective hydrogenation of nitro compounds with supported gold catalysts. *Science* **313**, 332–334 (2006). doi:10.1126/science.1128383 Medline
4. M. Sankar, N. Dimitratos, P. J. Miedziak, P. P. Wells, C. J. Kiely, G. J. Hutchings, Designing bimetallic catalysts for a green and sustainable future. *Chem. Soc. Rev.* **41**, 8099–8139 (2012). doi:10.1039/c2cs35296f Medline
5. H. M. Torres Galvis, J. H. Bitter, C. B. Khare, M. Ruitenbeek, A. I. Dugulan, K. P. de Jong, Supported iron nanoparticles as catalysts for sustainable production of lower olefins. *Science* **335**, 835–838 (2012). doi:10.1126/science.1215614 Medline

6. W. Luo, M. Sankar, A. M. Beale, Q. He, C. J. Kiely, P. C. A. Bruijnincx, B. M. Weckhuysen, High performing and stable supported nano-alloys for the catalytic hydrogenation of levulinic acid to γ-valerolactone. *Nat. Commun.* **6**, 6540 (2015). doi:10.1038/ncomms7540 Medline
7. J. Zečević, G. Vanbutsele, K. P. de Jong, J. A. Martens, Nanoscale intimacy in bifunctional catalysts for selective conversion of hydrocarbons. *Nature* **528**, 245–248 (2015). doi:10.1038/nature16173 Medline
8. M. D. Hughes, Y.-J. Xu, P. Jenkins, P. McMorn, P. Landon, D. I. Enache, A. F. Carley, G. A. Attard, G. J. Hutchings, F. King, E. H. Stitt, P. Johnston, K. Griffin, C. J. Kiely, Tunable gold catalysts for selective hydrocarbon oxidation under mild conditions. *Nature* **437**, 1132–1135 (2005). doi:10.1038/nature04190 Medline
9. P. Munnik, P. E. de Jongh, K. P. de Jong, Recent developments in the synthesis of supported catalysts. *Chem. Rev.* **115**, 6687–6718 (2015). doi:10.1021/cr500486u Medline
10. F. Tao, *Metal Nanoparticles for Catalysis: Advances and Applications* (Royal Society of Chemistry, 2014).
11. E. M. van Schrojenstein Lantman, T. Deckert-Gaudig, A. J. G. Mank, V. Deckert, B. M. Weckhuysen, Catalytic processes monitored at the nanoscale with tip-enhanced Raman spectroscopy. *Nat. Nanotechnol.* **7**, 583–586 (2012). doi:10.1038/nnano.2012.131 Medline
12. G. Prieto, J. Zečević, H. Friedrich, K. P. de Jong, P. E. de Jongh, Towards stable catalysts by controlling collective properties of supported metal nanoparticles. *Nat. Mater.* **12**, 34–39 (2013). doi:10.1038/nmat3471 Medline
13. R. V. Jagadeesh, A.-E. Surkus, H. Junge, M.-M. Pohl, J. Radnik, J. Rabeah, H. Huan, V. Schünemann, A. Brückner, M. Beller, Nanoscale Fe2O3-based catalysts for selective hydrogenation of nitroarenes to anilines. *Science* **342**, 1073–1076 (2013). doi:10.1126/science.1242005 Medline
14. R. V. Jagadeesh, H. Junge, M. Beller, Green synthesis of nitriles using non-noble metal oxides-based nanocatalysts. *Nat. Commun.* **5**, 4123 (2014). doi:10.1038/ncomms5123 Medline
15. H. Furukawa, K. E. Cordova, M. O'Keeffe, O. M. Yaghi, The chemistry and applications of metal-organic frameworks. *Science* **341**, 1230444 (2013). doi:10.1126/science.1230444 Medline
16. A. Corma, H. García, F. X. Llabrés i Xamena, Engineering metal organic frameworks for heterogeneous catalysis. *Chem. Rev.* **110**, 4606–4655 (2010). doi:10.1021/cr9003924 Medline
17. H. Wang, Q.-L. Zhu, R. Zou, Q. Xu, Metal-Organic Frameworks for Energy Applications. *Chem* **2**, 52–80 (2017). doi:10.1016/j.chempr.2016.12.002
18. P. Pachfule, D. Shinde, M. Majumder, Q. Xu, Fabrication of carbon nanorods and graphene nanoribbons from a metal-organic framework. *Nat. Chem.* **8**, 718–724 (2016). doi:10.1038/nchem.2515 Medline
19. J. Tang, Y. Yamauchi, Carbon materials: MOF morphologies in control. *Nat. Chem.* **8**, 638–639 (2016). doi:10.1038/nchem.2548 Medline
20. W. Xia, A. Mahmood, R. Zou, Q. Xu, Metal–organic frameworks and their derived nanostructures for electrochemical energy storage and conversion. *Energy Environ. Sci.* **8**, 1837–1866 (2015). doi:10.1039/C5EE00762C
21. K. Shen, X. Chen, J. Chen, Y. Li, Development of MOF-Derived Carbon-Based Nanomaterials for Efficient Catalysis. *ACS Catal.* **6**, 5887–5903 (2016). doi:10.1021/acscatal.6b01222
22. X. Ma, Y.-X. Zhou, H. Liu, Y. Li, H.-L. Jiang, A MOF-derived Co-CoO@N-doped porous carbon for efficient tandem catalysis: Dehydrogenation of ammonia borane and hydrogenation of nitro compounds. *Chem. Commun. (Camb.)* **52**, 7719–7722 (2016). doi:10.1039/C6CC03149H Medline
23. B. Liu, H. Shioyama, T. Akita, Q. Xu, Metal-organic framework as a template for porous carbon synthesis. *J. Am. Chem. Soc.* **130**, 5390–5391 (2008). doi:10.1021/ja7106146 Medline
24. S. A. Lawrence, *Amines: Synthesis, Properties and Applications* (Cambridge University Press, 2004).
25. A. Ricci, *Amino Group Chemistry: From Synthesis to the Life Sciences* (Wiley-VCH, Weinheim, 2008).
26. http://njardarson.lab.arizona.edu/sites/njardarson.lab.arizona.edu/files/Top200Pharmaceutical ProductsRetailSales2015LowRes.pdf.
27. S. D. Roughley, A. M. Jordan, The medicinal chemist's toolbox: An analysis of reactions used in the pursuit of drug candidates. *J. Med. Chem.* **54**, 3451–3479 (2011). doi:10.1021/jm200187y Medline
28. P. M. Dewick, *Medicinal Natural Products: A Biosynthetic Approach* (3rd Edn, Wiley, 2008).
29. C. Joyce, W. F. Smyth, V. N. Ramachandran, E. O'Kane, D. J. Coulter, The characterisation of selected drugs with amine-containing side chains using electrospray ionisation and ion trap mass spectrometry and their determination by HPLC-ESI-MS. *J. Pharm. Biomed. Anal.* **36**, 465–476 (2004). doi:10.1016/j.jpba.2004.07.026 Medline
30. S. Gomez, J. A. Peters, T. Maschmeyer, The Reductive Amination of Aldehydes and Ketones and the Hydrogenation of Nitriles: Mechanistic Aspects and Selectivity Control. *Adv. Synth. Catal.* **344**, 1037–1057 (2002). doi:10.1002/1615-4169(200212)344:10<1037:AID-ADSC1037>3.0.CO;2-3
31. H. Alinezhad, H. Yavari, F. Salehian, Recent Advances in Reductive Amination Catalysis and Its Applications. *Curr. Org. Chem.* **19**, 1021–1049 (2015). doi:10.2174/1385272819666150311233021
32. V. N. Wakchaure, J. Zhou, S. Hoffmann, B. List, Catalytic asymmetric reductive amination of α-branched ketones. *Angew. Chem. Int. Ed.* **49**, 4612–4614 (2010). doi:10.1002/anie.201001715 Medline
33. D. Chusov, B. List, *Angew. Chem. Int. Ed.* **53**, 5199–5201 (2014).
34. S. Ogo, K. Uehara, T. Abura, S. Fukuzumi, pH-Dependent chemoselective synthesis of α-amino acids. Reductive amination of α-keto acids with ammonia catalyzed by acid-stable iridium hydride complexes in water. *J. Am. Chem. Soc.* **126**, 3020–3021 (2004). doi:10.1021/ja031633r Medline
35. Y. Nakamura, K. Kon, A. S. Touchy, K.-i. Shimizu, W. Ueda, Selective Synthesis of Primary Amines by Reductive Amination of Ketones with Ammonia over Supported Pt catalysts. *ChemCatChem* **7**, 921–924 (2015). doi:10.1002/cctc.201402996
36. T. Gross, A. M. Seayad, M. Ahmad, M. Beller, Synthesis of primary amines: First homogeneously catalyzed reductive amination with ammonia. *Org. Lett.* **4**, 2055–2058 (2002). doi:10.1021/ol0200605 Medline
37. P. Ryberg, R. Berg, U.S. patent WO2015/178846 A1, 2015.
38. J. Gallardo-Donaire, M. Ernst, O. Trapp, T. Schaub, Direct Synthesis of Primary Amines *via* Ruthenium-Catalysed Amination of Ketones with Ammonia and Hydrogen. *Adv. Synth. Catal.* **358**, 358–363 (2016). doi:10.1002/adsc.201500968
39. G. Liang, A. Wang, L. Li, G. Xu, N. Yan, T. Zhang, Production of Primary Amines by Reductive Amination of Biomass-Derived Aldehydes/Ketones. *Angew. Chem. Int. Ed.* **56**, 3050–3054 (2017). doi:10.1002/anie.201610964 Medline
40. Z. Wang, Ed., Mignonac Reaction, in *Comprehensive Organic Name Reactions and Reagents* (Wiley, 2010).
41. F. Mao, D. Sui, Z. Qi, H. Fan, R. Chen, J. Huang, Heterogeneous cobalt catalysts for reductive amination with $H_2$: General synthesis of secondary and tertiary amines. *RSC Advances* **6**, 94068–94073 (2016). doi:10.1039/C6RA21415K
42. F. Santoro, R. Psaro, N. Ravasio, F. Zaccheria, Reductive Amination of Ketones or Amination of Alcohols over Heterogeneous Cu Catalysts: Matching the Catalyst Support with the N-Alkylating Agent. *ChemCatChem* **4**, 1249–1254 (2012). doi:10.1002/cctc.201200213
43. T. Stemmler, A.-E. Surkus, M.-M. Pohl, K. Junge, M. Beller, Iron-catalyzed synthesis of secondary amines: On the way to green reductive aminations. *ChemSusChem* **7**, 3012–3016 (2014). doi:10.1002/cssc.201402413 Medline
44. R. V. Jagadeesh, T. Stemmler, A.-E. Surkus, H. Junge, K. Junge, M. Beller, Hydrogenation using iron oxide-based nanocatalysts for the synthesis of amines. *Nat. Protoc.* **10**, 548–557 (2015). doi:10.1038/nprot.2015.025 Medline
45. S. Pisiewicz, T. Stemmler, A.-E. Surkus, K. Junge, M. Beller, Synthesis of Amines by Reductive Amination of Aldehydes and Ketones using $Co_3O_4$/NGr@C Catalyst. *ChemCatChem* **7**, 62–64 (2015). doi:10.1002/cctc.201402527
46. T. Stemmler, F. A. Westerhaus, A.-E. Surkus, M.-M. Pohl, K. Junge, M. Beller, General and selective reductive amination of carbonyl compounds using a core–shell structured $Co_3O_4$/NGr@C catalyst. *Green Chem.* **16**, 4535–4540 (2014). doi:10.1039/C4GC00536H


Downloaded from http://science.sciencemag.org/ on September 21, 2017

47. P. Zhou, Z. Zhang, L. Jiang, C. Yu, K. Lv, J. Sun, S. Wang, A versatile cobalt catalyst for the reductive amination of carbonyl compounds with nitro compounds by transfer hydrogenation. *Appl. Catal. B* **210**, 522–532 (2017). doi:10.1016/j.apcatb.2017.04.026
48. J. W. Park, Y. K. Chung, Hydrogen-Free Cobalt–Rhodium Heterobimetallic Nanoparticle-Catalyzed Reductive Amination of Aldehydes and Ketones with Amines and Nitroarenes in the Presence of Carbon Monoxide and Water. *ACS Catal.* **5**, 4846–4850 (2015). doi:10.1021/acscatal.5b01198
49. F. Buchner, K. Flechtner, Y. Bai, E. Zillner, I. Kellner, H.-P. Steinrück, H. Marbach, J. M. Gottfried, Coordination of Iron Atoms by Tetraphenylporphyrin Monolayers and Multilayers on Ag(111) and Formation of Iron-Tetraphenylporphyrin. *J. Phys. Chem. C* **112**, 15458–15465 (2008). doi:10.1021/jp8052955
50. F. Jaouen, J. Herranz, M. Lefèvre, J.-P. Dodelet, U. I. Kramm, I. Herrmann, P. Bogdanoff, J. Maruyama, T. Nagaoka, A. Garsuch, J. R. Dahn, T. Olson, S. Pylypenko, P. Atanassov, E. A. Ustinov, Cross-laboratory experimental study of non-noble-metal electrocatalysts for the oxygen reduction reaction. *ACS Appl. Mater. Interfaces* **1**, 1623–1639 (2009). doi:10.1021/am900219g Medline
51. http://www.nwafs.org/newsletters/SyntheticAmphetamine.pdf.
52. M. Feng, B. Tang, S. H. Liang, X. Jiang, Sulfur containing scaffolds in drugs: Synthesis and application in medicinal chemistry. *Curr. Top. Med. Chem.* **16**, 1200–1216 (2016). doi:10.2174/1568026615666150915111741 Medline
53. E. J. Barreiro, A. E. Kümmerle, C. A. M. Fraga, The methylation effect in medicinal chemistry. *Chem. Rev.* **111**, 5215–5246 (2011). doi:10.1021/cr200060g Medline
54. J. Chatterjee, F. Rechenmacher, H. Kessler, *N*-methylation of peptides and proteins: An important element for modulating biological functions. *Angew. Chem. Int. Ed.* **52**, 254–269 (2013). doi:10.1002/anie.201205674 Medline
55. R. Quanqing, Z. Tingjian, W. Shaojie, China patent CN 101735201A (2010).
56. Y. Zhang, Y. Liu, Z. Song, Y. Zhu, G. Gao, China patent CN 104788326 (2016).
57. E. W. Baxter, A. B. Reitz, ''Reductive Aminations of Carbonyl Compounds with Borohydride and Borane Reducing Agents'' in *Organic Reactions*, Wiley (2004)
58. S. A. Forsyth, H. Q. N. Gunaratne, C. Hardacre, A. McKeown, D. W. Rooney, One-Pot Multistep Synthetic Strategies for the Production of Fenpropimorph Using an Ionic Liquid Solvent. *Org. Process Res. Dev.* **10**, 94–102 (2006). doi:10.1021/op050172m
59. J.-C. Souvie, U.S. patent US5142053A (1992).
60. B. Lal, S. Lahiri, C. P. Bapat, R. S. Kulkarni, D. K. Mulla, A. Y. Hawaldar, U.S. patent WO2010046908A2 (2010).

## ACKNOWLEDGMENTS

We gratefully acknowledge the support of European Research Council (ERC), Federal Ministry of Education and Research (BMBF), the State of Mecklenburg-Vorpommern and King Abdulaziz City for Science and Technology (KACST). We thank the analytical staff of the Leibniz-Institute for Catalysis, Rostock for their excellent service. All data are available in Supplementary Materials.

## SUPPLEMENTARY MATERIALS

www.sciencemag.org/cgi/content/full/science.xxxxxxx/DC1
www.sciencemag.org/cgi/content/full/science.aan6245/DC1
Materials and Methods
Figs. S1 to S14
NMR and HRMS spectra

10 May 2017; accepted 7 September 2017
Published online 21 September 2017
10.1126/science.aan6245

Downloaded from http://science.sciencemag.org/ on September 21, 2017

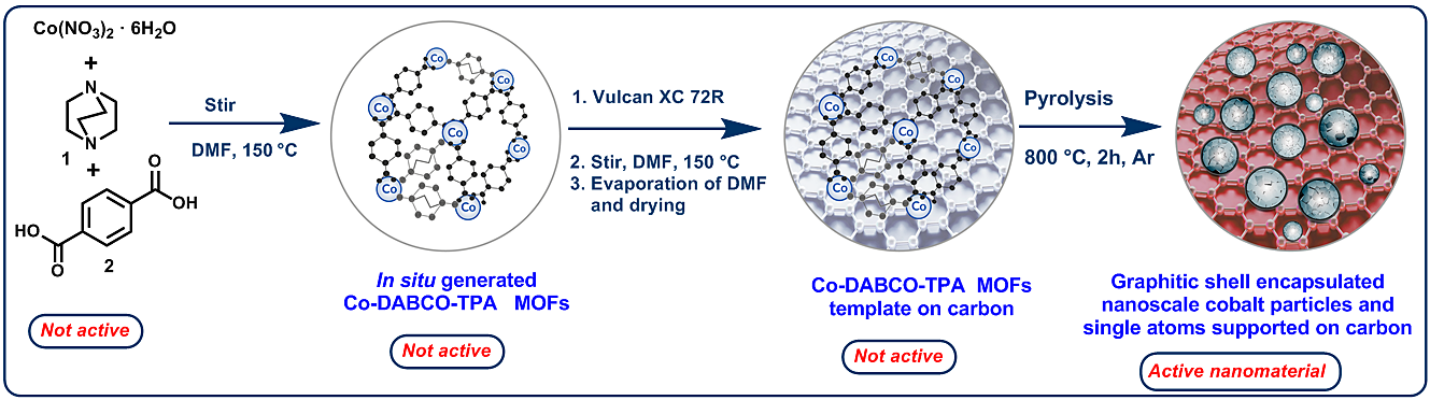


Fig. 1. Preparation of graphitic shell encapsulated cobalt nanoparticles supported on carbon using MOF precursors.

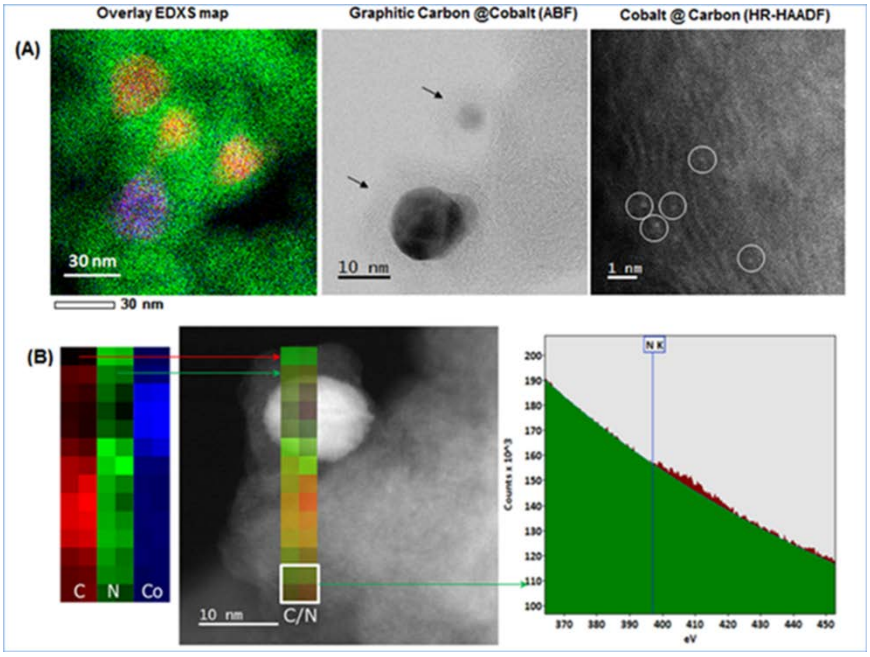


Fig. 2. Catalyst characterization. (A) EDXS map and STEM images of Co-DABCO-TPA@C-800 catalyst. EDXS map (left image): Cobalt = red, Oxygen = blue, Carbon = green. Black arrows highlight graphite embedded metallic Co particles (Middle image). White circles represent single Co atoms at carbon (right image). (B) EELS/EDXS study of Co-DABCO-TPA@C-800 catalyst. Left image= Parallel detected space-resolved Carbon (EELS), Nitrogen (EELS) and Cobalt (EDX) signals. Middle image = HAADF image overlaid by C/N elemental map at the position of measurement. Right image= Nitrogen K-edge EELS- spectrum of the white box in the middle image.

Downloaded from http://science.sciencemag.org/ on September 21, 2017

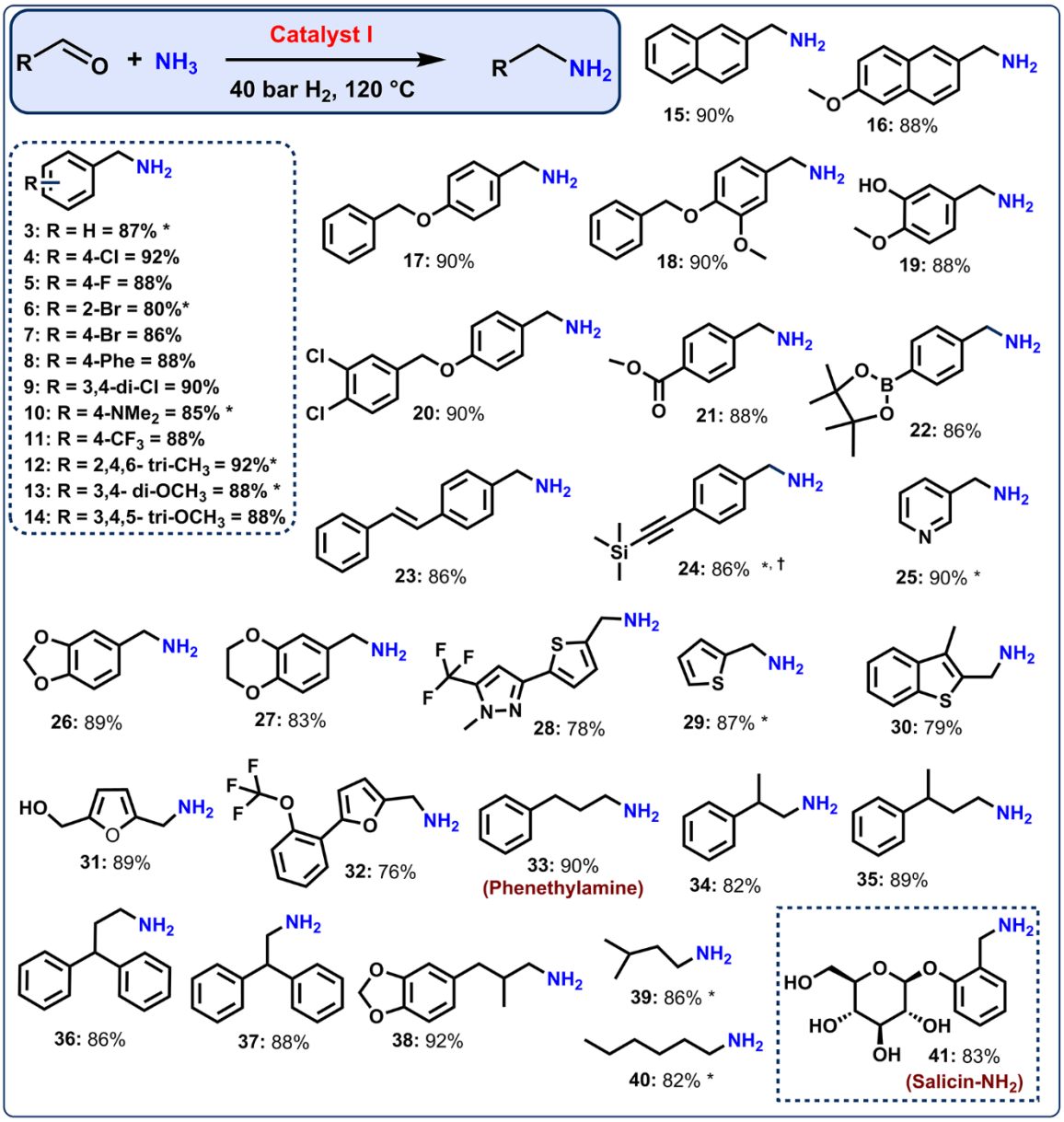


**Fig. 3. Co-DABCO-TPA@C-800 catalyzed reductive amination of aldehydes for the synthesis of linear primary amines.** Reaction conditions: 0.5 mmol aldehyde, 25 mg catalyst **I** (3.5 mol % Co), 5-7 bar $NH_3$, 40 bar $H_2$, 3 mL *t*-BuOH, 120°C, 15 hours; isolated yields reported unless otherwise indicated. *GC yields using n-hexadecane standard. † 8 hours. Isolated as free amines and converted to hydrochloride salts for measuring NMR and HRMS spectra.

Downloaded from http://science.sciencemag.org/ on September 21, 2017

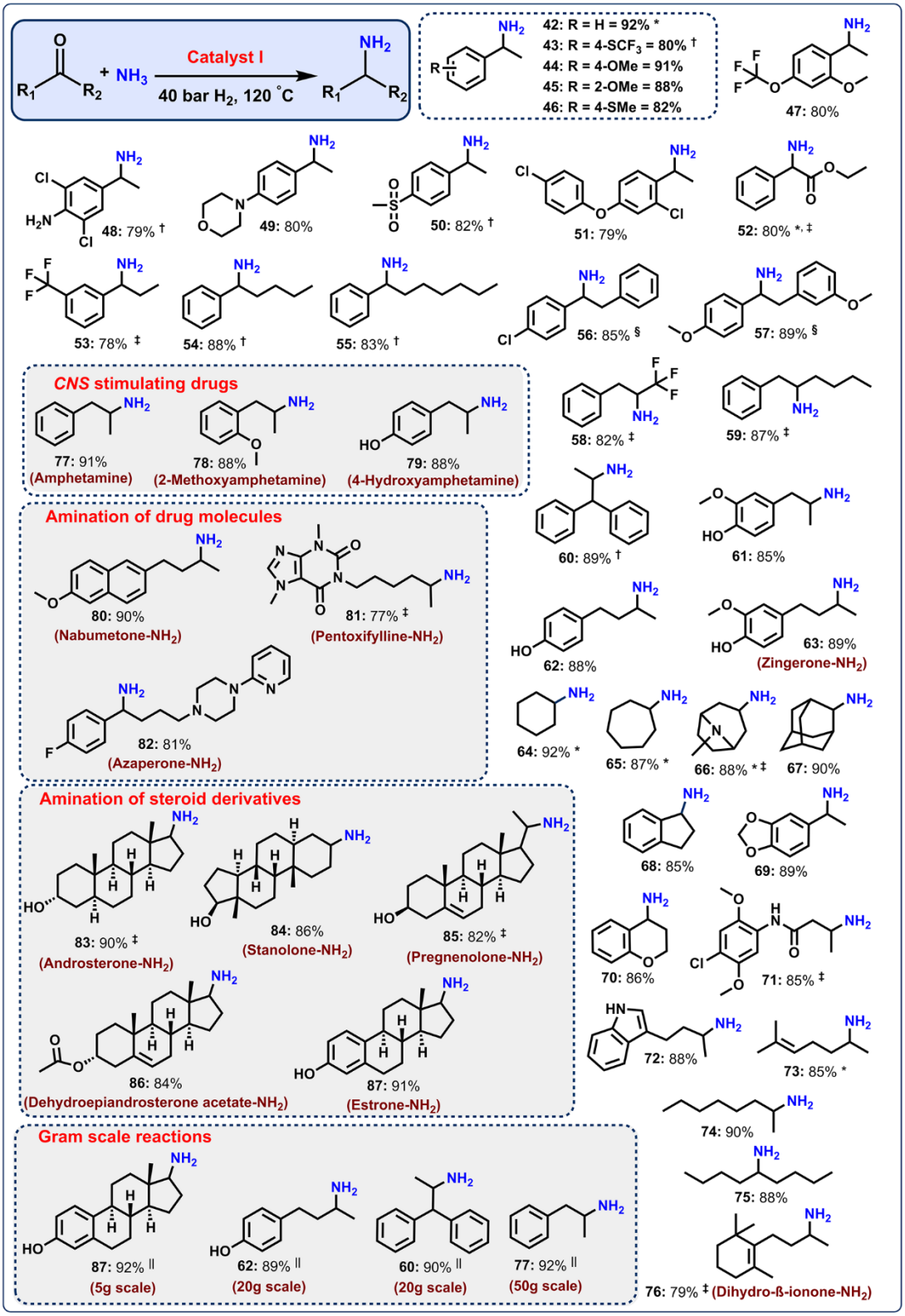


**Fig. 4. Co-DABCO-TPA@C-800 catalyzed reductive amination of ketones.** Reaction conditions: 0.5 mmol ketone, 25 mg catalyst **I** (3.5 mol % Co), 5-7 bar $NH_3$, 40 bar $H_2$, 3 mL THF (dry), 120°C, 15 hours; isolated yields reported unless otherwise indicated. *GC yields using n-hexadecane standard. †For 20 hours. ‡For 24 hours. § For 30 hours with 35 mg catalysts. Isolated as free amines and converted to hydrochloride salts for measuring NMR and HRMS. ||5-50 g substrate, 25 mg catalyst **I** (3.5 mol% Co) for each 0.5 mmol substrate, 5-7 bar $NH_3$, 40 bar $H_2$, 120-150 mL dry THF, 120°C, 15-30 hours, isolated yields.

Downloaded from http://science.sciencemag.org/ on September 21, 2017

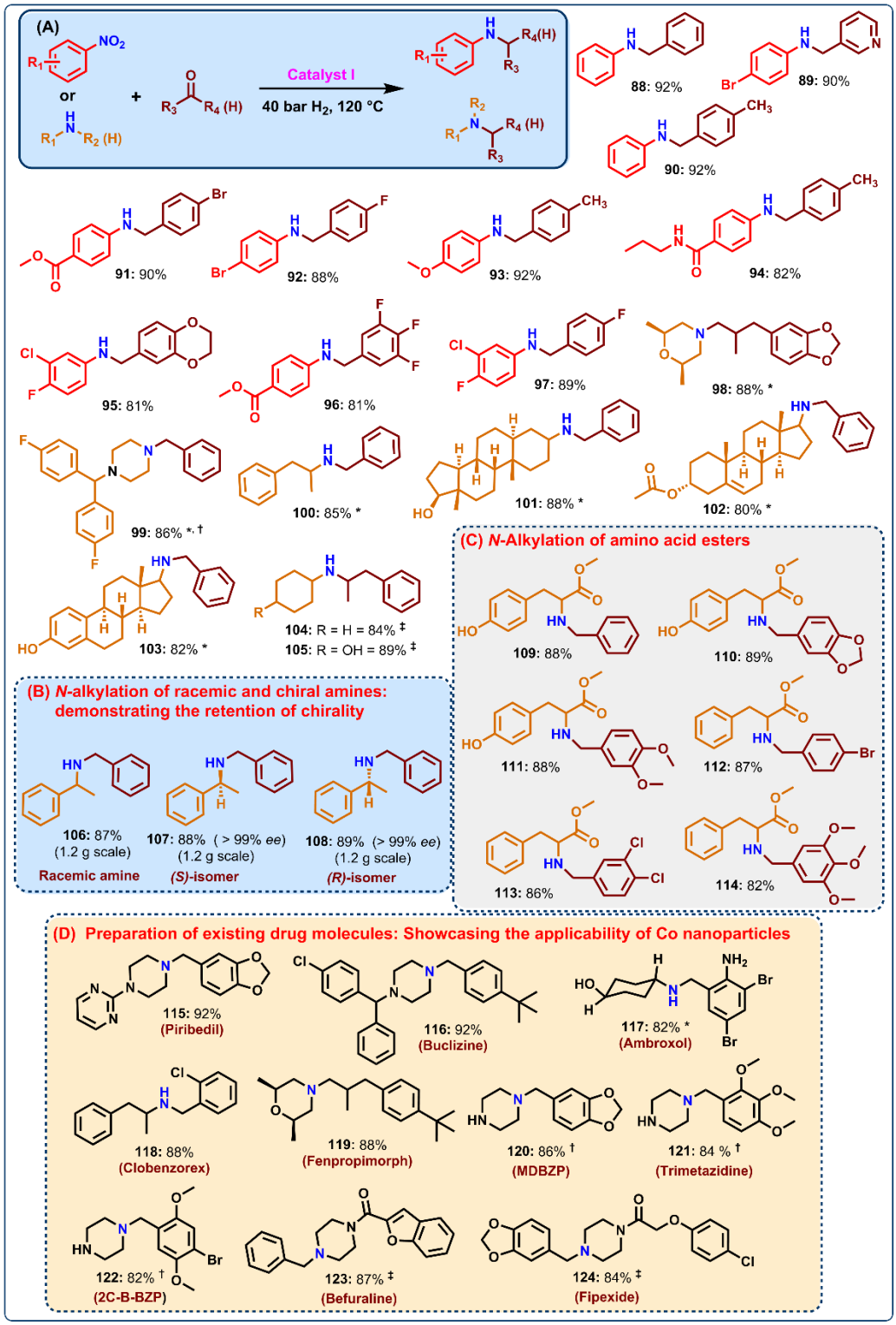


**Fig. 5. Co-DABCO-TPA@C-800 catalyzed synthesis of secondary and tertiary amines.** (**A**) Survey of nitroarenes and amines. Reaction conditions: 0.5 mmol nitroarene, 0.75-1 mmol aldehyde, 25 mg catalyst **I** (3.5 mol % Co), 20 mg amberlite IR-120, 3 mL *t*-BuOH, 120°C, 24 hours; isolated yields. *0.5 mmol amine, 0.75 mmol aldehyde. † 30 mg catalyst, 30h. ‡0.5 mmol amine, 0.75 mmol ketone. (**B**) Reductive *N*-alkylation of chiral amines. Reaction conditions: 10 mmol amine, 15 mmol benzaldehyde, 500 mg catalyst **I** (3.5 mol% Co), 400 mg amberlite IR-120, 15 mL *t*-BuOH, 120°C, 24 hours; isolated yields. (**C**) Reductive *N*-alkylation of amino acid esters. Reaction conditions: 0.5 mmol amino acid ester, 0.75 mmol aldehyde, 25 mg catalyst (3.5 mol% Co), 20 mg amberlite IR-120, 3 mL *t*-BuOH, 120°C, 24 hours; isolated yields. (**D**) Preparation of existing drug molecules. Reaction conditions: 1 mmol amine, 1.5 mmol aldehyde, 50 mg catalyst **I** (3.5 mol % Co), 3 mL *t*-BuOH, 120°C, 24 hours; isolated yields. *75 mg catalyst for 30 hours. †2 mmol amine, 1 mmol aldehyde. ‡Synthesis same as (†) followed by acylation with acid chlorides (see supplementary materials S6.5. for detailed procedure).

Downloaded from http://science.sciencemag.org/ on September 21, 2017

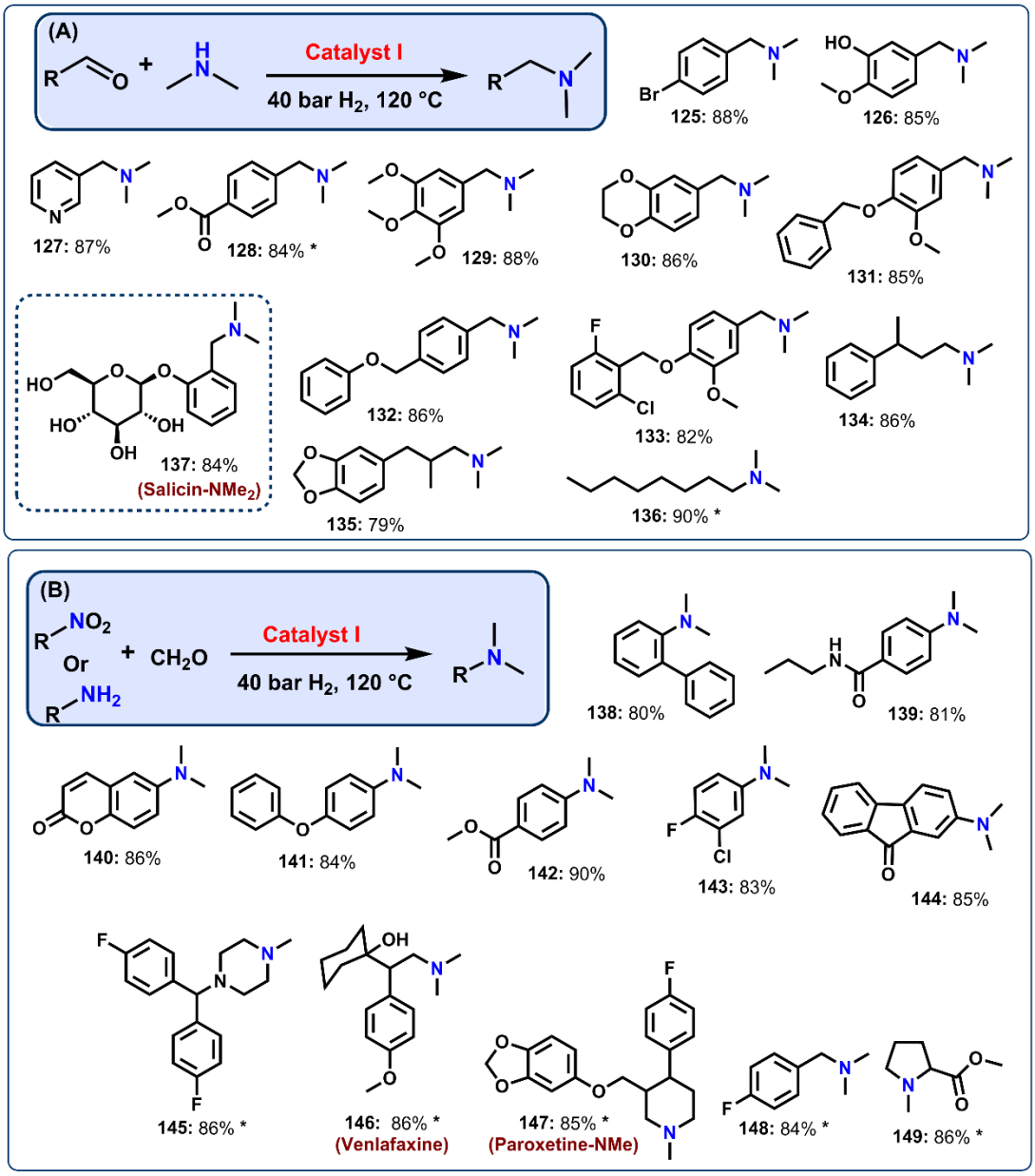


**Fig. 6. Co-DABCO-TPA@C-800 catalyzed preparation of *N*-methylamines.** (**A**) Reactions of aldehydes with dimethylamine. Conditions: 0.5 mmol aldehyde, 100 µL aqueous dimethylamine (40%), 25 mg catalyst **I** (3.5 mol % Co), 3 mL *t*-BuOH, 120°C, 24 hours; isolated yields yields reported unless otherwise indicated. *GC yields using n-hexane standard. (**B**) Reactions of nitroarenes or amines with formaldehyde. Conditions: 0.5 mmol nitroarene, 100-200 µL aqueous formaldehyde (37%), 1:1 THF- $H_2O$ (3mL); isolated yields. *0.5 mmol amine, 100-200 µL aqueous formaldehyde (37%), 1:1 THF- $H_2O$ (3 mL).

Downloaded from http://science.sciencemag.org/ on September 21, 2017

Science

# MOF-derived cobalt nanoparticles catalyze a general synthesis of amines

Rajenahally V. Jagadeesh, Kathiravan Murugesan, Ahmad S. Alshammari, Helfried Neumann, Marga-Martina Pohl, Jörg Radnik and Matthias Beller

published online September 21, 2017

**ARTICLE TOOLS** http://science.sciencemag.org/content/early/2017/09/20/science.aan6245

**SUPPLEMENTARY MATERIALS** http://science.sciencemag.org/content/suppl/2017/09/20/science.aan6245.DC1

**REFERENCES** This article cites 45 articles, 4 of which you can access for free
http://science.sciencemag.org/content/early/2017/09/20/science.aan6245#BIBL

**PERMISSIONS** http://www.sciencemag.org/help/reprints-and-permissions

Use of this article is subject to the Terms of Service

*Science* (print ISSN 0036-8075; online ISSN 1095-9203) is published by the American Association for the Advancement of Science, 1200 New York Avenue NW, Washington, DC 20005. 2017 © The Authors, some rights reserved; exclusive licensee American Association for the Advancement of Science. No claim to original U.S. Government Works. The title *Science* is a registered trademark of AAAS.

Downloaded from http://science.sciencemag.org/ on September 21, 2017